Smart Structures and Systems, Vol. 9, No. 5 (2012) 461-472
DOI: http://dx.doi.org/10.12989/sss.2012.9.5.461

Damage detection for pipeline structures using optic-based active sensing

Hyeonseok Lee and Hoon Sohn*

Department of Civil and Environmental Engineering, Korea Advanced Institute of Science and Technology, Daejeon 305-701, Korea

(Received July 26, 2011, Revised April 19, 2012, Accepted April 20, 2012)

Abstract. This study proposes an optics-based active sensing system for continuous monitoring of underground pipelines in nuclear power plants (*NPPs*). The proposed system generates and measures guided waves using a single laser source and optical cables. First, a tunable laser is used as a common power source for guided wave generation and sensing. This source laser beam is transmitted through an optical fiber, and the fiber is split into two. One of them is used to actuate macro fiber composite (*MFC*) transducers for guided wave generation, and the other optical fiber is used with fiber Bragg grating (*FBG*) sensors to measure guided wave responses. The *MFC* transducers placed along a circumferential direction of a pipe at one end generate longitudinal and flexural modes, and the corresponding responses are measured using *FBG* sensors instrumented in the same configuration at the other end. The generated guided waves interact with a defect, and this interaction causes changes in response signals. Then, a damage-sensitive feature is extracted from the response signals using the axi-symmetry nature of the measured pitch-catch signals. The feasibility of the proposed system has been examined through a laboratory experiment.

Keywords: guided waves; structural health monitoring (*SHM*); macro fiber composite (*MFC*) transducer; fiber Bragg grating (*FBG*) sensor; laser; nuclear power plant; pipeline structures

1. Introduction

It has been reported that the structural integrity of pipeline facilities in nuclear power plants (*NPPs*) continues to deteriorate and it may pose a serious problem (IAEA 2009). Considering the significance of *NPPs*, there is a strong desire to develop an online structural health monitoring (*SHM*) system that enables continuous and automatic monitoring of *NPPs* to complement current nondestructive testing (*NDT*) technology. In particular, among various kinds of components in *NPPs*, underground pipelines might be best suited for continuous *SHM* due to their lack of accessibility in spite of vulnerability to structural defects. There are several types of underground pipelines in *NPPs*: service water, diesel fuel oil, fire protection, emergency feedwater, and condenser recirculating water (Braverman *et al.* 2005). Structural damage in these underground pipeline systems can cause detrimental consequences. Even a small defect can result in paralysis of the entire *NPP* system, and it can sometimes pose a serious safety risk through a leak of radioactive water. Therefore, the Nuclear Regulatory Commission (*NRC*) of the US government has requested

*Corresponding author, Professor, E-mail: hoonsohn@kaist.ac.kr

researchers worldwide to propose proper inspection techniques for assuring the integrity of underground pipelines in *NPPs* (NEI 2010).

One of the promising techniques for pipeline inspection is guided wave techniques, because they have a long wave propagation distance through a pipe and a high sensitivity to small defects (Victorov 1967, Rose *et al*. 1996, Lowe *et al*. 1998, Inman 2005). Devices commonly used for generation and measurement of guided waves in pipeline structures include electro-magnetic acoustic transducer (*EMAT*) (Böttger *et al*. 1987), magnetostrictive transducer (Kwun *et al*. 2003, Kim *et al*. 2005), ring-shaped transducer module (Lowe *et al*. 1998, Demma *et al.* 2003), and pulse laser ultrasonics devices (Lee *et al.* 2009) to name a few. However, these devices are mainly designed for periodic *NDT* rather than continuous *SHM*, and the data collected from these measurement systems often have to be analyzed by trained inspection personnel.

One of the best embeddable devices for continuous *SHM* might be macro fiber composite (*MFC*) transducers and fiber Bragg grating (*FBG*) sensors due to their negligible mass/volume, non-intrusive nature and flexibility (Sodano *et al*. 2004, Su *et al*. 2006). However, *MFC* transducers are basically made of a mixture of lead zirconite titanate (*PZT*) and polymer materials and inherited some of the problems associated with conventional *PZT* materials such as susceptibility to electromagnetic interference (*EMI*) and reliance on conventional copper wires. *EMI* is known to induce distortion of response signals and false alarm indications of damage (Dai *et al*. 2009, Wu *et al*. 2009), and data transmitted over conventional cables suffer from noise contamination and signal attenuation especially for a long range transmission. *FBG* sensing addresses these problems because optical fibers are less susceptible to noise, less vulnerable to power attenuation and immune to *EMI*. However, they are only applicable to guided wave sensing due to their intrinsic passive nature (Wu *et al.* 2009). To overcome these shortcomings, several researchers have developed hybrid measurement systems. For example, combinations of *PZT*-based guided wave actuation and *FBG*-based sensing have been attempted (Betz *et al*. 2003, Qing *et al*. 2005, Tsuda 2006). However, these hybrid approaches cannot take a full advantage of the merits of optical fibers since electrical cablings are still required for the excitation of the *PZT* transducers.

This study develops a truly integrated active sensing system that uses only optical devices, such as a laser beam and optical fibers, for guided wave excitation and sensing. Furthermore, a unique damage detection algorithm based on axi-symmetry nature of guided wave propagation paths is developed to enable robust damage detection under varying environmental conditions.

2. Working principles

Fig. 1 shows the schematic overview of the proposed hybrid active sensing system. A similar hybrid scheme has been developed by the authors using a *PZT* transducer for guided wave generation (Lee *et al*. 2010). Because conventional *PZT* transducers are brittle and not conformable to curved surfaces, *MFC* transducers are used in this study for guided wave generation in pipes. Furthermore, a laser beam is used to simultaneously excite multiple *MFC* transducers to create axi-symmetric longitudinal modes. One major difference between *MFC* and *PZT* transducers is that, while the *PZT* transducer produces bi-directional in-plane excitations, the *MFC* generates excitation primarily in one direction. In this study, the primary axis of the *MFC* excitation is aligned along the longitudinal direction of the pipe. In the proposed measurement system, a tunable laser is used as a common power source for both guided wave generation and sensing. The laser beam is divided into two

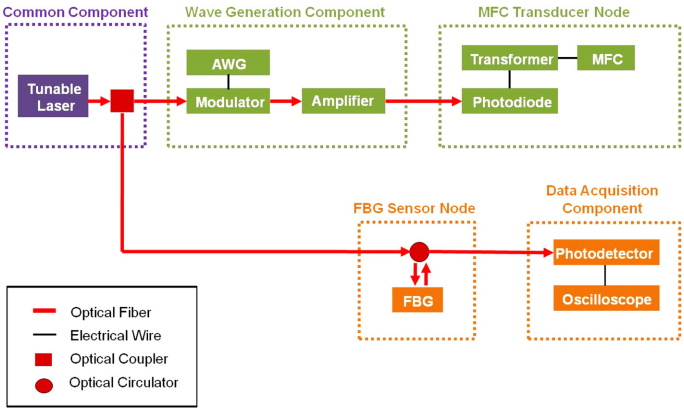

Fig. 1 Schematic overview of the proposed hybrid guided wave generation and sensing system

beams by using an optical coupler. As for guided wave generation, the laser beam is modulated using an optical modulator in accordance with the target waveform from the arbitrary waveform generator (*AWG*). Then, the modulated laser beam is amplified by a fiber amplifier to meet the power requirement for *MFC* actuation. When the laser beam is transmitted to the *MFC* excitation node, multiple *MFC* transducers are simultaneously excited and guided waves are generated in a pipe specimen. The other laser beam divided from the optical coupler is incident on the *FBG* sensor and then reflected back at a specific wavelength. The intensity change of the reflected laser beam at the *FBG*'s wavelength is related to the dynamic strain induced by the propagating guided waves (Fisher *et al*. 1998). Each process will be explained in detail in the following subsections.

2.1 Guided wave generation using MFC transducers

The tunable laser beam has a continuous waveform. To realize an active sensing scheme, a proper modulation process is required to transform the intensity of the laser beam into a desired waveform. The first step in guided wave excitation is to create a desired input waveform using the *AWG*. A seven-peak toneburst signal, which is commonly used for guided wave based damage detection, is employed as a reference signal throughout this study.

Then, the reference signal is exerted to the optical modulator, and the modulator modulates the power intensity of the tunable laser beam in accordance with the reference signal. The principle of the optical modulator is based on electro-optic effects (Wilson *et al*. 1998). As the electric field produced by the reference signal is applied across an optical medium, the polarizability and the refractive index of the medium vary, resulting in the light intensity change.

Fig. 2 shows the intrinsic transfer function of the optical modulator, and its intrinsic nonlinear nature. The tunable laser beam is modulated with respect to the applied voltage. A localized linear relationship between the input voltage and the output light intensity is achieved by limiting the perturbation range of the input voltage. A *DC* bias is added to the input voltage to shift the zero level of the reference signal to a 50% light intensity level (Kasap 2001, Khare 2004).

By biasing the input voltage during the modulation process, the transmission rate decreases and the laser beam attenuates more. To increase the level of the output laser beam power, this system utilizes an erbium-doped fiber amplifier. Then, a photodiode and a pn junction-typed transformer

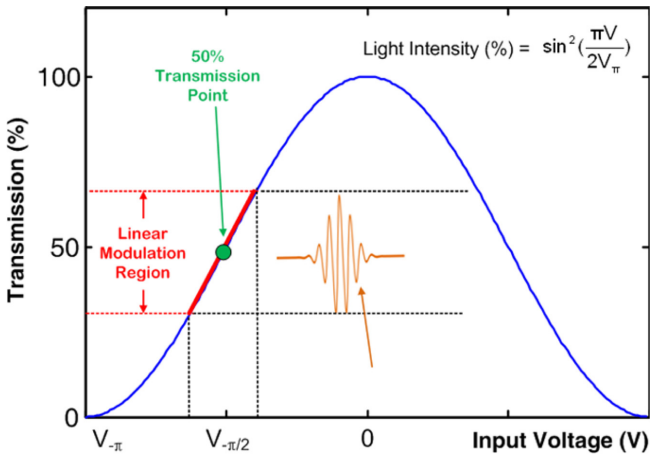

Fig. 2 Transfer function of the optical modulator

convert the laser beam into electrical signals to actuate the *MFC* transducers (Park *et al*. 2011). Even though a *MFC* transducer does not require high level of electrical power, it needs a certain level of voltage to generate guided waves (Greve *et al.* 2007). Since the photodiode generates the photocurrent output with a low level of voltage, a transformer is used to increase the voltage level.

2.2 Guided wave sensing using an FBG sensor

A *FBG* is a periodic and permanent variation in the refractive index of a fiber core. A *FBG* acts as an optical filter that reflects light only in a certain narrow bandwidth centered around the Bragg wavelength λ_B. The first-order approximation of the fractional change in the Bragg wavelength $\frac{\Delta\lambda_B}{\lambda_B}$ is given as follows

$$\frac{\Delta\lambda_B}{\lambda_B} = C_\varepsilon \varepsilon \tag{1}$$

where ε is the applied strain, and C_ε is a constant that depends on material properties (Bass *et al.* 2002). This equation indicates that the measurement of $\Delta\lambda_B$ can be related to the dynamic strain changes induced by guided waves.

Fig. 3 shows the transfer functions of the *FBG* sensor and the tunable laser to explain the working principle of the optical interrogation method (Betz *et al.* 2003). The transfer function of the *FBG* sensor has a bell-shaped distribution centered around the Bragg wavelength λ_B. When the structure is subjected to dynamic strain as shown in Figs. 3(b) and (c), the whole *FBG* transfer function shifts horizontally. On the other hand, the transfer function of the tunable laser is much narrower than that of the *FBG* sensor, and the central wavelength of the transfer function is fixed at a certain value throughout the measurement process. When the tunable laser launches light to the *FBG* sensor, some of the incident light is reflected. The optical intensity of the reflected light, the *FBG*'s reflectivity, is proportional to the overlapped area between the *FBG* and tunable laser transfer functions. Therefore, the strain change in the *FBG* sensor causes the horizontal shift of the *FBG* transfer function and subsequently the variation of the *FBG* reflectivity. The linear relationship between the strain change and the *FBG* reflectivity is guaranteed by keeping the peak of the tunable laser transfer

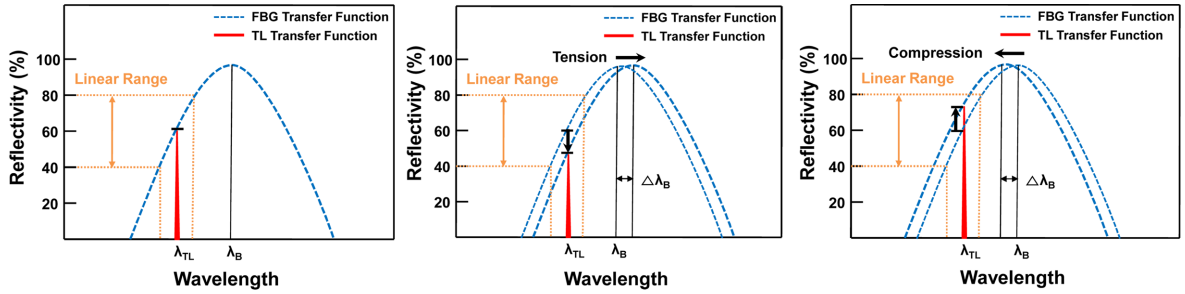

Fig. 3 Variation in reflectivity of the tunable laser beam with strain changes: (a) Initially, the peak of the tunable laser (*TL*) transfer function, λ_{TL}, is positioned in the middle of a linear range of the *FBG* transfer function at a strain-free condition, (b) as the *FBG* is subjected to tension, the *FBG* transfer function moves to the right and the reflectivity at λ_{TL} decreases and (c) as the *FBG* is subjected to compression, the *FBG* transfer function moves to the left and the reflectivity at λ_{TL} increases.

function, λ_{TL}, to fall within the wavelength range of the *FBG* transfer function corresponding to 40~80% of the grating's maximum reflectivity (Betz *et al*. 2003, Tsuda *et al*. 2006).

2.3 Damage detection approach

Besides developing an embeddable hybrid system for active sensing, this study also proposes a robust damage detection algorithm for pipeline monitoring. The proposed damage detection scheme extracts a feature, which is sensitive to damage but insensitive to environmental variation, from the measured guided wave responses based on the symmetry of wave propagation paths in a pipeline structure. Note that extracting of environment invariant damage feature is important because pipelines in *NPPs* are subjected to a variation in ambient vibration and temperature.

Fig. 4 shows the configuration of *MFC* transducers and *FBG* sensors used for the proposed damage diagnosis. For guided wave excitation, multiple *MFC* transducers ("group A": A_1, A_2, ..., A_n), which are equally spaced in a circumferential direction, are attached at one end of the pipe. Similarly, multiple *FBG* sensors ("group B": B_1, B_2, ..., B_n) are placed at the other end of the pipe. Here, n is an arbitrary number, and this number can be increased to improve damage detectability. In this study, four *MFC* transducers and four *FBG* sensors are used. For guided wave generation, all "group A" transducers are simultaneously excited so that mainly longitudinal (*L*) modes can be generated while suppressing the excitation of other low-order dominant flexural (*F*) modes. For guided wave sensing, the response at each *FBG* sensor in the "group B" is recorded one at a time,

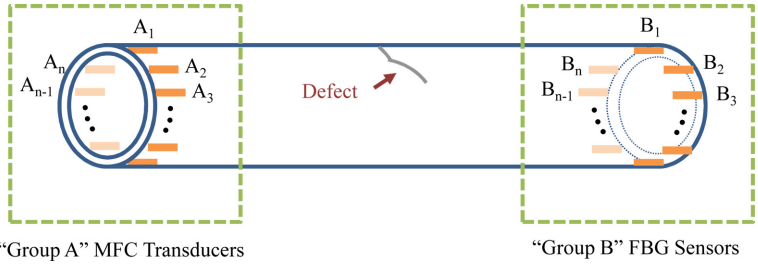

Fig. 4 *MFC* and *FBG* configuration for the proposed damage diagnosis of a pipe structure

Table 1 Notation of wave paths

Wave path	Excitation point	Sensing point
AB_1	Group A	B_1
AB_2	Group A	B_2
…	…	…
AB_n	Group A	B_n

producing a total of n wave propagation paths as shown in Table 1.

Due to the axi-symmetric nature of a pipe, all Signal AB_i (i=1,2,...,n) should be, in theory, identical at the intact condition. This equality breaks down when a non-axisymmetric defect is introduced. Based on this observation, the following damage index can be obtained in a round-robin fashion

$$DI(i, j)=RMS \text{ (Signal } AB_i \text{ - Signal } AB_j) \text{ for } i \neq j \quad (2)$$

where *RMS* denotes a root-mean-square, and a total of $n(n\text{-}1)/2$ damage index values can be obtained for n wave paths. The value of the damage index will be close to zero for an intact case, but it will increase for a damage case.

3. Experimental setup

Fig. 5 shows the carbon steel pipe specimen used in this experiment, which has a length of 528 mm, an outer diameter of 114.3 mm and a thickness of 6 mm, respectively. In this experiment, four *MFC* transducers are attached at one end of the specimen, and four *FBG* sensors, which are 400 mm away from the *MFC* transducers in the longitudinal direction, are placed at the other end of the specimen. The *MFC* transducers (M-2814-P1, Smart-Material) are expansion-type, and their dimensions are 28 mm×14 mm. The four *FBG* sensors have different Bragg wavelengths of 1544 nm, 1546 nm, 1548 nm and 1550 nm, respectively. They have a grating length of 10 mm and use a single mode optical fiber. As for structural damage, a circumferential notch was engraved 200 mm away from the *MFC* transducers (Fig 6) to simulate crack damage. In this experiment, the notch has a circumferential length of 40 mm and a depth of 2 mm.

The proposed system mainly consists of five subcomponents: a common laser source, wave generation

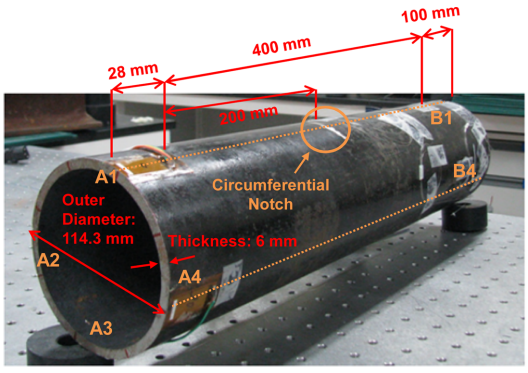

Fig. 5 Test specimen for the experiment

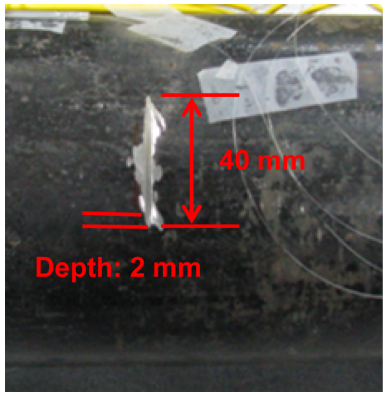

Fig. 6 Circumferential notch

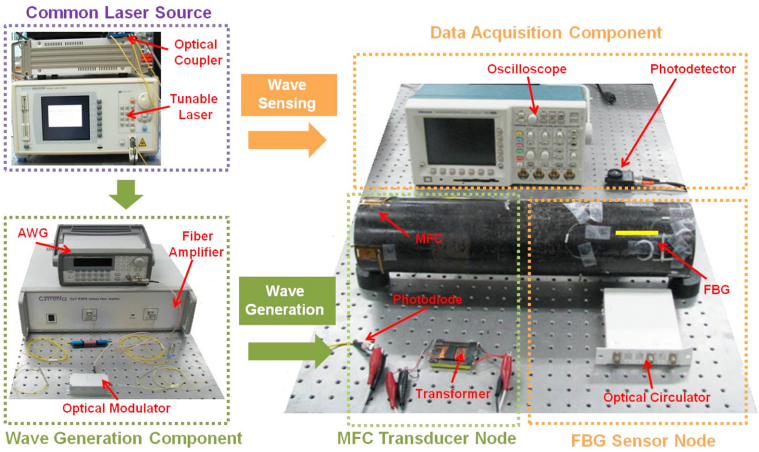

Fig. 7 Overall configuration of the experimental setup

component, *MFC* transducer node, *FBG* sensor node, and data acquisition component (Fig. 7). In the common laser source, the power level of the tunable laser (AQ4321A, *ANDO*) is set to 2.0 mW and the laser beam is divided into two: one for generation and the other for sensing of guided waves. In the wave generation component, a toneburst signal with 3 V peak-to-peak voltage and a driving frequency of 130 kHz is generated using the AWG (33220A, Agilent). Then, this toneburst waveform is exerted to the optical modulator for amplitude modulation of the tunable laser beam. The modulated laser beam power is amplified up to a maximum of 200 mW using the fiber amplifier and transmitted through the optical fiber. A single-mode optical fiber (*SMF*-28) was used for laser beam transmission. At the *MFC* transducer node, the optical power of the laser beam is converted to electrical current by using the InGaAs-typed photodiode (*FGA*04, Thorlabs). Finally, the transformer increases the voltage level of the converted electrical current up to 20 times to simultaneously excite the four *MFC* transducers. Finally, the guided waves propagate through the specimen and the generated guided waves are measured using the *FBG* sensors. To measure the guided waves using the *FBG* sensors, the other tunable laser beam divided by the optical coupler is delivered to the *FBG* sensor. The laser beam reflected from the *FBG* sensors is redirected to the data acquisition

component using the optical circulator (Agiltron), converted to the electrical signal using the photodetector (*PDA* 10CS-EC, Thorlabs) and displayed on the oscilloscope (*TDS* 30254B, Tektronix) in the data acquisition component. The sampling rate of the data acquisition component is 25 MHz/sec.

4. Experimental results

4.1 Guided wave generation

Fig. 8 shows the comparison between the reference and input signals. For the comparison of the two signals, a seven peak toneburst signal with a central frequency of 130 kHz and a peak-to-peak voltage of 3 V is used as the reference signal. The input signal, which is the voltage actually applied to the *MFC* transducer, has a peak-to-peak voltage of 10.8 V and a central frequency of 125.7 kHz. These two signals are normalized for better comparison so that their peak-to-peak values become ±1. The comparison of these two signals reveals that the input signal is delayed about 0.525 μsec with respect to the reference signal, and the shape of the input signal is altered from that of the reference signal. The discrepancy between the two signals is quantitatively computed using the following equation

$$\rho_{X,Y} = \frac{\mathrm{cov}(X,Y)}{\sigma_X \sigma_Y} = \frac{E[(X-\mu_X)(Y-\mu_Y)]}{\sigma_X \sigma_Y} \tag{3}$$

where X and Y are the original reference and input signals. μ_X and μ_Y are the mean values of X and Y, and σ_X and σ_Y are the standard deviations of X and Y, respectively. The cross-correlation coefficient value between two signals is computed to be 0.7233. The distortion and delay in the input signal are attributed to several factors: non-linear nature of the optical modulator, time delay in the *pn* junction-typed photodiode, and time delay in the transformer. However, it should be noted that we are not so much concerned with the difference between the input and reference signals for damage diagnosis. Our main interest is to make sure that we can apply a consistent input each time and measure the change of the response signal due to damage. The issue of minimizing the difference between the input and reference signals is discussed in Lee *et al.* (2010).

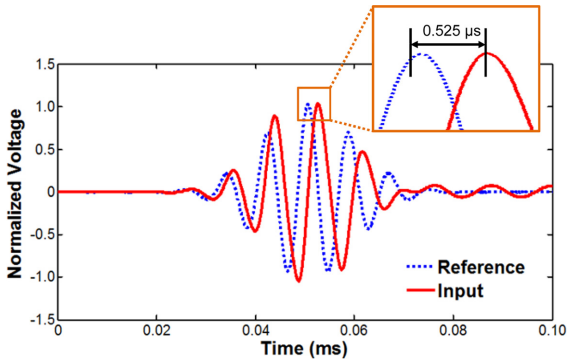

Fig. 8 Time delay and signal distortion of the input signal with respect to the reference signal

4.2 Guided wave measurement

Fig. 9 shows the response signals measured at four *FBG* sensors (i.e., Signal AB_1, Signal AB_2, Signal AB_3 and Signal AB_4) from the intact and damage conditions. Each response signal is normalized so that the maximum absolute value of each signal becomes one. In the response signal, the first wave packet is clearly observed, but the second wave packet is superposed with reflections. Also, the response signals from the intact and damage cases show little discrepancy. The cross-correlation coefficient between the response signals from the intact and damage conditions varies from 0.8 to 1.0 for Signal AB_1, Signal AB_2, Signal AB_3 and Signal AB_4. This indicates that successful damage diagnosis cannot be achieved simply by comparing the cross-correlation between

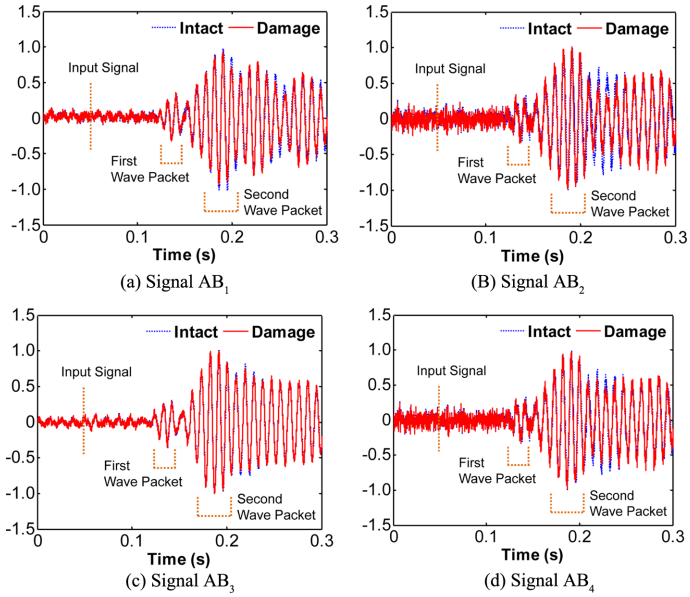

Fig. 9 Comparison of the guided wave response signals obtained from the intact (dotted line) and damage (solid line) conditions

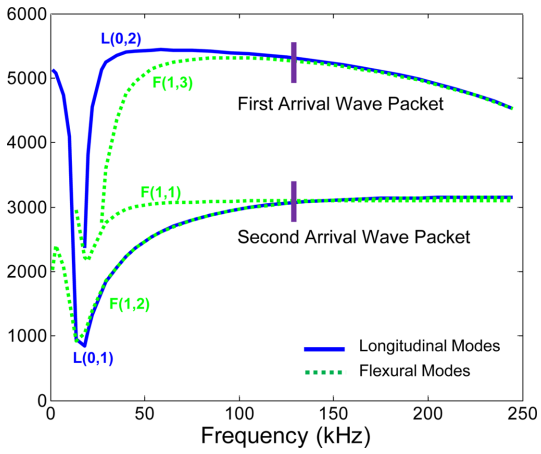

Fig. 10 Group velocities of cylindrical wave modes in the pipe specimen

the intact and damage cases.

To examine the measured response signals, the time-of-flight of each signal is compared with the theoretical value. Fig. 10 shows the dispersion curve of the target pipeline specimen. Since the pipe specimen is almost axi-symmetrically excited using the four *MFC* transducers, there are two governing wave groups: (1) $L(0,1)$ mode and the adjacent flexural modes, and (2) $L(0,2)$ mode and the adjacent flexural modes. The first and second wave packets in each response signal correspond to these two wave groups. Considering the 400 mm distance between the *MFC* transducers and the *FBG* sensors, the theoretical arrival times of the group (1) and (2) waves are 0.0769 ms and 0.129 ms, respectively. These theoretical arrival times of these two group waves well match with the arrival times of the first and second wave packets observed in Fig. 9.

4.3 Damage detection

Fig. 11 shows the extracted damage feature as discussed in 2.3. Since we used four *MFC* transducers and four *FBG* sensors in this experiment, there are four wave paths (AB_1, AB_2, AB_3, and AB_4) and six damage index values. The damage index has non-zero values even for the intact case mainly due to the imperfect alignment and attachment of *MFC* transducers and *FBG* sensors. However, the intact case consistently has lower damage index values compared to the damage case.

The values of the damage index defined in Eq. (2) are computed in Table 2 for the intact and

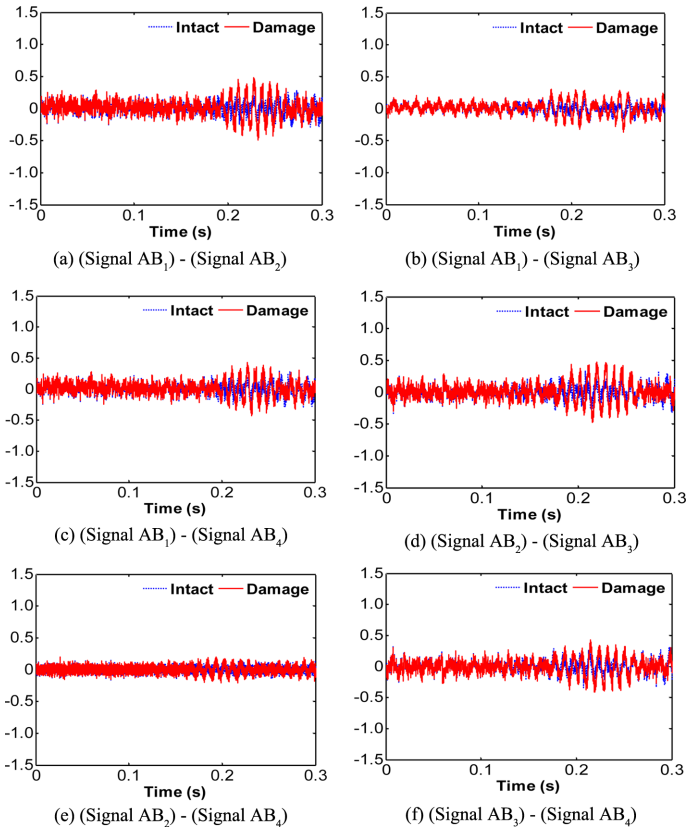

Fig. 11 Extracted damage feature from the measured signals

Table 2 Damage index

Damage index	Intact case	Damage case
DI (1,2)	0.0817	0.1505
DI (1,3)	0.0621	0.1161
DI (1,4)	0.0908	0.1292
DI (2,3)	0.0868	0.1602
DI (2,4)	0.0543	0.0717
DI (3,4)	0.1021	0.1418

damage cases. Note that a small value is obtained for *DI* (2,4) even for the damage case because two wave paths, AB_2 and AB_4, are almost symmetrically positioned with respect to the circumferential notch. The damage diagnosis performance can be further improved by increasing the power level of the tunable laser beam and thus increasing the signal-to-noise ratio of the *FBG* sensing.

5. Conclusions

This study develops a new guided wave excitation and sensing system and a damage detection technique specifically designed for underground pipelines. The proposed guided wave measurement system uses *MFC* transducers for guided wave generation and *FBG* sensors for sensing. The uniqueness of the proposed measurement system lies in that power and data needed for *MFC* excitation and *FBG* sensing are all optically transmitted using laser beam and optical cables, making this measurement system attractive for online *SHM* of long range underground pipes with readily embeddable *MFC* transducers and *FBG* sensors. Furthermore, a damage index specifically designed for damage diagnosis of a pipeline structure is proposed in this study. Experimental tests performed on a pipeline specimen indicate that guided waves can be successfully generated and recorded by the developed measurement system and the proposed damage index can be a good indicator of circumferential notch damage in a pipe. A further study is underway to develop a damage detection algorithm that can be built up on the proposed damage index for autonomous online *SHM* of pipes.

Acknowledgements

This research was supported by Mid-career Researcher Program and National Nuclear R&D Program through the National Research Foundation of Korea (NRF) funded by the Ministry of Education, Science and Technology (No. 2011-0016470 and No. 2011-0018430), and by the Innovations in Nuclear Power Technology (Development of Nuclear Energy Technology) of the Korea Institute of Energy Technology Evaluation and Planning (KETEP) grant funded by the Knowledge Economy (No. 2010T100101057) in Korea.

References

Bass, M. and Stryland, E.W.V. (2002), *Fiber optics handbook*, McGraw-Hill, New York.

Betz, D.C. and Thursby, G. (2003), "Acousto-ultrasonic sensing using fiber Bragg gratings", *Smart Mater. Struct*., **12**(1), 122-128.
Böttger, W., Schneider, H. and Weingarten, W. (1987), "Prototype EMAT system for tube inspection with guided ultrasonic waves", *Nucl. Eng. Des*., **102**(3), 369-376.
Braverman, J.I., DeGrassi, G., Martinez-Guridi, G., Morante, R.J. and Hofmayer, C.H. (2005), *Risk-informed assessment of degraded buried piping systems in nuclear power plants*, Brookhaven National Laboratory, Washington D.C.
Dai, Y., Liu, Y., Leng, J., Deng, G. and Asundi, A. (2009), "A novel time-division multiplexing fiber Bragg grating sensor interrogator for structural health monitoring", *Opt. Laser. Eng*., **47**(10), 1028-1033.
Greve, D., Sohn, H., Yue, P. and Oppenheim, I.J. (2007), "An inductively-coupled Lamb wave transducer", *IEEE Sens. J*., **7**(2), 295-301.
IAEA (2009), *Ageing management for nuclear power plants*, Safety Guide No. NS-G-2.12.
Inman, D.J. (2005), *Damage prognosis for aerospace*, Civil and Mechanical Systems, Wiley, Chichester.
Kasap, S.O. (2001), *Optoelectronics and photonics: principles and practices*, Prentice Hall, New Jersey.
Khare, R.P. (2004), *Fiber optics and optoelectronics*, Oxford University Press, Oxford.
Kim, Y.Y., Park, C.I., Cho, S.H. and Han, S.W. (2005), "Torsional wave experiments with a new magnetostrictive transducer configuration", *J. Acoust. Soc. Am*., **117**(6), 3459-3468.
Kwun, H., Kim, S.Y. and Light, G. (2003), "The magnetostrictive sensor technology for long range guided wave testing and monitoring of structures", *Mater. Eval*., **61**(1), 80-84.
Lee, H., Park, H.J., Sohn, H. and Kwon, I.B. (2010), "Integrated guided wave generation and sensing using a single laser source", *Meas. Sci. Technol*., **21**(10), 105207.
Lee, J.H. and Lee, S.J. (2009), "Application of laser-generated guided wave for evaluation of corrosion in carbon steel pipe", *NDT&E Int*., **42**(3), 222-227.
Lowe, M.J.S., Alleyne, D.N. and Cawley, P. (1998), "Defect detection in pipes using guided waves", *Ultrasonics*, **36**(1-5), 147-154.
Nuclear Energy Institute (2009), *Guideline for the management of underground piping and tank integrity*, Nuclear Energy Institute, Washington D.C.
Park, H.J., Sohn, H., Yun, C.B., Chung, J. and Lee, M. (2011), "Wireless guided wave and impedance measurement using laser and piezoelectric transducers", Submitted to IEEE Transactions on Ultrasonics, Ferroelectrics and Frequency Control.
Qing, X., Kumar, A., Zhang, C., Gonzalez, I.F., Guo, G. and Chang, F.K. (2005), "A hybrid piezoelectric/fiber optic diagnostic system for structural health monitoring", *Smart Mater. Struct*., **14**(3), 98-103.
Rose, J.L., Jiao, D. and Spanner, Jr. J. (1996), "Ultrasonic guided wave NDE for piping", *Mater. Eval*., **54**(11), 1310-1313.
Sodano, H.A., Park, G. and Inman, D.J (2004), "An investigation into the performance of macro-fiber composites for sensing and structural vibration applications", *Mech. Syst. Signal Pr*., **18**(3), 683-697.
Su, Z., Ye, L. and Lu, Y. (2006), "Guided Lamb waves for identification of damage in composite structures: A review", *J. Sound Vib*., **295**(3-5), 753-780.
Tsuda, H. (2006), "Ultrasound and damage detection in CFRP using fiber Bragg grating sensors", *Compos. Sci. Technol*., **66**(5), 676-683.
Victorov, I.A. (1967), *Rayleigh and lamb waves-physical theory and applications*, Plenum, New York.
Wilson, J. and Hawkes, J. (1998), *Optoelectronics: An introduction*, Prentice Hall, New Jersey.
Wu, Z., Qing, X.P. and Chang, F.K. (2009), "Damage detection for composite laminate plates with a distributed hybrid PZT/FBG sensor network", *J. Intell. Mater. Syst. Struct*., **20**(9), 1069-1077.

CC